pn-type substrate dependence of CsK$_2$Sb photocathode performance

L. Guo[*] and M. Katoh

UVSOR Facility, Institute for Molecular Science, National Institutes of Natural Sciences,
38 Nishigo-Naka, Myodaiji, Okazaki 444-8585, Japan

The CsK$_2$Sb photocathode is capable of generating a high-intensity and low-emittance electron beam with visible laser light. In this study, we examined CsK$_2$Sb photocathode evaporation on *n*- and *p*-type Si(100), GaAs(100), and Si(111) substrates, and compared their cathode performance. We found that the quantum efficiency of the *p*-type substrate was superior to that of the *n*-type substrate for the same substrate material and surface orientation. We show that this can be qualitatively analyzed by an energy-band model for the semiconductor(metal)-semiconductor junction between CsK$_2$Sb and the substrate. We also evaporated the Cs$_3$Sb cathode on *n*- and *p*-type Si(100) and GaAs(100) substrates, and confirmed that the cathode performance of all substrates was consistent with the model results. This finding indicates the possibility of improving the thin-film cathode performance by revisiting the semiconductor(metal)-semiconductor junction between the cathode and the substrate, which improves the understanding of high-performance photocathodes.

I. INTRODUCTION

Future accelerator projects based on linear accelerators, such as the Energy Recovery Linac (ERL) [1], Free Electron Laser (FEL) [2], and Linear Collider (LC) [3] will extend the knowledge base in scientific applications. Photocathodes are one of the most important subsystems in advanced linear accelerators because the accelerator performance strongly depends on the initial beam quality. For example, in the baseline design of the LCLS II project [4], which is the first continuous wave x-ray FEL project in the United States, a large current up to 0.3 mA is required with 0.4 mm · mrad emittance.

Since the 1980s, photocathodes have been operated in many accelerators [5]. The most popular photo-cathode materials are metals such as Cu [6] or Ag [7]. To generate an intense electron beam against the low quantum efficiency (QE) of photoelectron emissions, typically in the order of 0.01%, and the large work function, a high-power UV laser is required, which may be produced by harmonic generations [8] but with low efficiency.

The negative electron affinity-GaAs cathode has excellent properties such that the QE can be higher than 20% with the infrared (IR) laser. However, the negative electron affinity surface is fragile and easily damaged by residual gas adsorption or beam extraction.

Alkali (Multi) antimonide photocathodes composed of one or more alkali metals, such as Cs$_3$Sb and CsK$_2$Sb, are widely used in photomultiplier tubes [9]. The Cs$_3$Sb is normally a *p*-type material [10] and has high QE(1%–5%) with visible lasers [11].

CsK$_2$Sb is a nearly intrinsic semiconductor [12] fabricated as a thin film using the vacuum evaporation technique. The material can be driven by visible green light (532 nm) for photoemissions with QE values higher than 10% [13,14]. The material is robust against a large emission current [15]. Owing to these characteristics, CsK$_2$Sb is one of the best candidates for a high-brightness electron source at a large current density [16,17].

Although it is well known that the CsK$_2$Sb cathode performance depends on the substrate material and surface conditions [13,18–21], the underlying physics has not been extensively studied to date because of the lack of standardization of the cathode evaporation process. For example, the dependence of the cathode performance on the surface orientation of the CsK$_2$Sb or the substrate crystal was studied but not significantly observed [22,23] because the cathode evaporation condition was not fully optimized in these studies. Indeed, the QE in these studies was relatively low (3%).

Recently, it was shown that about 5% QE and nearly atomically smooth films of K-Cs-Sb could be obtained with good reproducibility by a triple-element co-deposition in which all three elements of K, Cs and Sb were evaporated simultaneously onto the substrate [24,25]. One the other hand, in our previous study, we established a cathode

[*]lguo@ims.ac.jp

evaporation process, which produced high QE with good reproducibility by the sequential evaporation of Sb, K and Cs on a substrate [26]. Based on this process, we proved that the cathode performance depends not only on cleanness and crystallinity, but also on the surface orientation of the crystalline substrate.

To improve our understanding for the underlying physics of CsK$_2$Sb photo-cathode, we studied the effect of the semiconductor type (p or n) of the substrates on the cathode performance. For this purpose, CsK$_2$Sb cathode was fabricated on Si(100), Si(111), and GaAs(100) of the p- and n-type with the process established in our previous study [26].

II. EXPERIMENT

The experimental setup was described in Ref. [26]. The cathode was fabricated in a vacuum chamber at a typical pressure of 1.0×10^{-8} Pa. The cathode substrate is fixed on a molybdenum puck. The puck is mounted on the cathode holder during evaporation and electron emissions. In this study, Si(100) and Si(111) p-type wafers with resistivity of $\leq 0.002\ \Omega$ cm, Si(100) and Si(111) n-type wafers with resistivity of $\leq 0.002\ \Omega$ cm, GaAs(100) p-type wafers with resistivity of $\leq 0.007\ \Omega$ cm and GaAs(100) n-type wafers with resistivity of $\leq 0.002\ \Omega$ cm were employed as the substrates.

The Si(100) and Si(111) substrates were processed with a 5% HF solution for 5 min [27] and the GaAs surface was processed with a H$_2$SO$_4$: H$_2$O$_2$: H$_2$O(4 : 1 : 1) solution for 5 min [28].

The CsK$_2$Sb cathode was formed by the sequential evaporation of Sb, K, and Cs on a substrate, which is summarized as follows. (1) The substrate was heated to 500–600 °C and held at that temperature for one hour to remove the surface oxidized layer (heat cleaning process). (2) The temperature was lowered to 100 °C. During evaporation, this temperature was maintained. (3) A 10 nm-thick layer of Sb was evaporated. (4) Then, K was evaporated. Simultaneously, QE was observed by illuminating the cathode with the 532 nm laser light. The evaporation was stopped when QE was saturated, which usually occurs between 0.3 and 1.0%. 5. The Cs layer was evaporated. The Cs evaporation was controlled in the same manner as that for the K evaporation. The QE was typically between 1 and 10%. 6. The substrate was cooled to room temperature.

An example of the QE evolution during the cathode evaporation is shown in Fig. 1 for the p-Si(100) substrates. Typically, QE on p-Si(100) was 9.8% at 532 nm laser. The laser spot size is 0.5 mm^2 and the cathode was biased at -100 V. The laser power was adjusted to 0.6 mW, and the typical photocurrent was 25 μA. The photocurrent was measured as the current of the bias supplier and the limit of photocurrent is 10 nA. The results (maximum QE) of all of substrates are summarized in Table I including the results
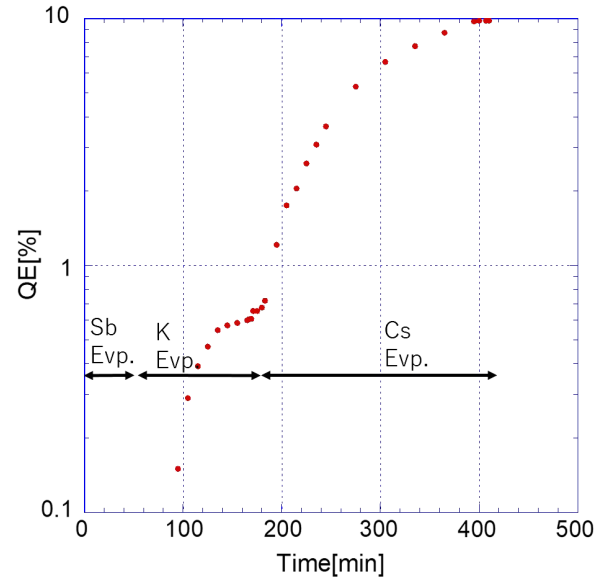

FIG. 1.   QE evolution during the evaporation process. Sb, K, and Cs was evaporated on p-type Si(100) substrate in this order. QE measured by 532 nm laser was launched during K evaporation and much enhanced in Cs evaporation.

of the previous studies. The evaporation was done on eight samples for each substrate type. The samples were heated to initialize the surface before each evaporation. We observed no photocurrent above the detection limit (10 nA) for the 400 nm laser after heating. The error was calculated as the standard deviation for the eight samples, indicating the high reproducibility of the evaporation process.

The QE of the Si(111) substrate was 1.6–2.8% at 532 nm. The p-Si(100) and p-GaAs(100) substrates showed a satisfactory QE as high as 10%. These results are similar to those of the Mo(100) [13] and Si(100) [14] substrates. The cathode performance of the p-type substrate was higher than that of n-type substrate with the same substrate surface orientation and material. This is the experimental evidence that the CsK$_2$Sb cathode performance depends on the pn-type of the substrate. The difference of CsK$_2$Sb cathode performance between Si

TABLE I.   The maximum QE of the CsK$_2$Sb photocathode on n-type Si(100), n-type Si(111), n-type GaAs(100), p-type Si (100), p-type Si(111), and p-GaAs(100) substrates at 532 nm.

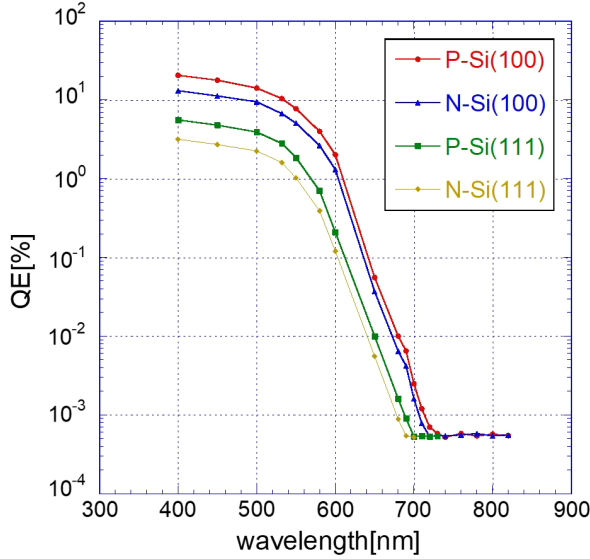| Substrate	QE[%]@532 nm
p-type GaAs(100)	10.1 ± 0.4
n-type GaAs(100)	7.0 ± 0.5
p-type Si(100)	9.7 ± 0.7
n-type Si(100)	6.7 ± 0.4
p-type Si(111)	2.8 ± 0.1
n-type Si(111)	1.6 ± 0.1
Mo(100)	10 [13]
p-type Si(100)	7–10[14]

FIG. 2. Spectral response for a CsK$_2$Sb photo-cathode, with red circles, blue triangles, green squares and yellow rhombuses for the *p*-Si(100), *n*-S(100), *p*-Si(111) and *n*-Si(111) substrates, respectively. The measurement limit of photocurrent is 10 nA.

(100) and Si(111) substrates is caused by the dependence on the substrate surface orientation [26].

After evaporating CsK$_2$Sb, we measured the spectral response of the photocathode as a function of the wavelength. A lamp (Asahi, High Power xenon lamp, MAX-303) and a monochromator (Asahi, Czerny-Turner type single monochromator, CMS-100) provided a variable wavelength light in the range of 400–900 nm with a typical bandwidth of 1%. Figures 2 and 3 show the spectral
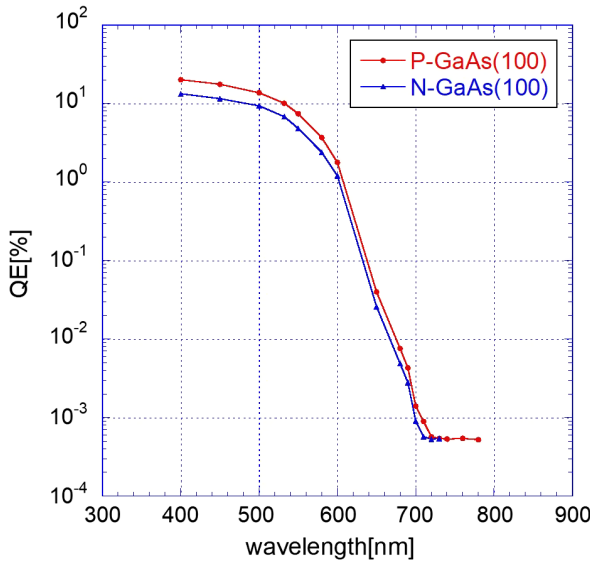

FIG. 3. Spectral response for a CsK$_2$Sb photo-cathode, with red circles and blue triangles for the *p*-GaAs(100) and *n*-GaAs(100) substrates, respectively. The measurement limit of photo-current is 10 nA.

TABLE II. The maximum QE values of the Cs$_3$Sb photocathode on *n*-type Si(100), *n*-type GaAs(100), *p*-type Si(100), and *p*-GaAs(100) substrates at 532 nm.

Substrate	QE[%]@532 nm
p type GaAs(100)	5.3 ± 0.2
n-type GaAs(100)	5.4 ± 0.3
p-type Si(100)	5.3 ± 0.2
n-type Si(100)	5.2 ± 0.2
p-Si(100)	4–5[30]

response of the CsK$_2$Sb photo-cathode on various substrates. QEs larger than 20% are obtained on *p*-Si(100) and *p*-GaAs(100) at 400 nm. These results are similar to those on the *p*-type Si(100) substrate obtained by the preceding studies [29].

We also evaporated Cs$_3$Sb on *p*-type Si(100), *n*-type Si(100), *p*-type GaAs(100), and *n*-type GaAs(100) substrates using the same process as CsK$_2$Sb but only 5 nm Sb. The results (maximum QE) of all substrates are summarized in Table II including the results of the preceding studies. The evaporation was done on eight samples for each substrate type. The error was calculated as the standard deviation for the eight samples. The QE of all the substrates was approximately 5.0% at 532 nm. These results are consistent with those of the preceding studies [30]. We did not observe the dependence of cathode performance on the pn-types of the substrates for Cs$_3$Sb.

III. DISCUSSION

The experimental results clearly show that the CsK$_2$Sb cathode performance depends on the *pn*-types of the substrates but this is not the case for Cs$_3$Sb. This is the first experimental evidence that photocathode performance can depend on the *pn*-types of the substrates.

CsK$_2$Sb is a direct transition type with 1.2 eV bandgap and 0.7 eV electron affinity [31]. CsK$_2$Sb is also a nearly intrinsic semiconductor [12]. CsK$_2$Sb and the substrate make the semiconductor(metal)-semiconductor junction. Fig. 4 shows the energy-band models for the junctions between CsK$_2$Sb and substrates, *p*-Si, *n*-Si, *p*-GaAs, *n*-GaAs and Mo. The vertical dashed line indicates the position of the substrate-cathode interface, and the area of the stripes shows the depletion region. By semiconductor (metal)-semiconductor junction, the energy band inside the cathode bends and the depletion region is formed. The conduction-band minimum of *p*-Si and *p*-GaAs are higher than that of CsK$_2$Sb and the conduction-band minimum of *n*-Si and *n*-GaAs are lower than that of CsK$_2$Sb.

In a previous x-ray reflectivity study [32], it was indicated that the CsK$_2$Sb photo-cathode is thicker by about a factor of 5 to 6 than that of evaporated Sb as in the case of the Cs$_2$Te cathode [33]. Therefore, the thickness of the photocathodes in this study may be around several tens
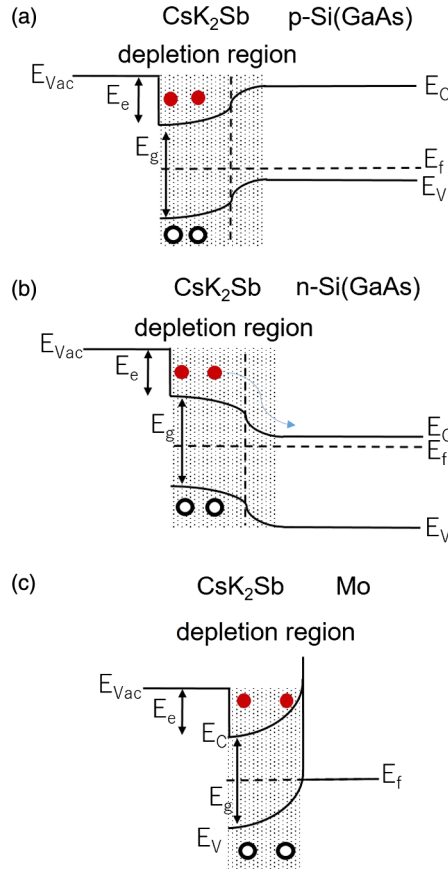
FIG. 4. The energy-band models for semiconductor(metal)-semiconductor junction between CsK_2Sb and substrates, (a) p-Si (GaAs), (b) n-Si(GaAs), (c) Mo. E_{Vac} is the vacuum level, E_C is the conduction band, E_V is the valence band, E_e is the electron affinity, E_g is the bandgap and E_f is the fermi level. The vertical dashed line indicates the position of the substrate-cathode interface, and the area of the stripes shows the depletion region.

FIG. 5. The energy-band models for semiconductor-semiconductor junction between Cs_3Sb and substrates, (a) p-Si(GaAs), (b) n-Si(GaAs). E_{Vac} is the vacuum level, E_C is the conduction band, E_V is the valence band, E_e is the electron affinity, E_g is the bandgap and E_f is the fermi level. The vertical dashed line indicates the position of the substrate-cathode interface, and the area of the stripes shows the depletion region.

of nanometers, which is larger than the photon penetration depth (about 20 nm). It is well known that the width of depletion region is typically several tens of nanometers even in heavily doped semiconductors and it is much wider in lightly doped or nearly intrinsic semiconductors [34]. We think that the CsK_2Sb photocathode is in the depletion region almost up to the surface, because CsK_2Sb is a nearly intrinsic semiconductor [12]. Due to the energy-band bending, the excited electrons in the depletion region cannot diffuse toward the substrates, p-Si and p-GaAs. On the other hand, they can easily diffuse toward the substrates, n-Si and n-GaAs. In this way, we can qualitatively understand why the quantum efficiency of the CsK_2Sb cathode on the n-type substrate is less than that on p-type substrate.

Figure 4(c) shows that the metal-semiconductor junction is similar to that between CsK_2Sb and p-type semiconductor substrates. The band bends upward on the CsK_2Sb cathode side and the excited electrons cannot diffuse toward the Mo side. For this reason, the CsK_2Sb cathode
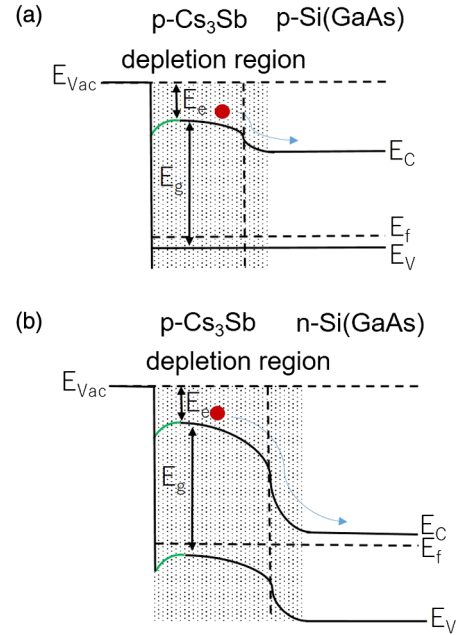
on the Mo substrate shows QE values as high as those on the p-type semiconductor substrates [13].

The cathode performance on n-Si(111) is smaller than that on other samples in this study because of the effect of the substrate surface orientation [26], in addition to the junction effect described above.

We found that the Cs_3Sb cathode performance of the substrates does not show a significant difference. This result also can be explained by the semiconductor-semiconductor junction between Cs_3Sb and the substrates. Cs_3Sb is a direct transition type semiconductor with 1.6 eV bandgap and 0.45 eV electron affinity [35]. It is well known that Cs_3Sb is a p-type semiconductor [10]. Figure 5 shows the energy-band models for the semiconductor-semiconductor junction between Cs_3Sb and the substrates, p-Si, n-Si, p-GaAs and n-GaAs. The vertical dashed line indicates the position of the substrate-cathode interface, and the area of the stripes shows the depletion region. The conduction-band minimum of all substrates are lower than that of Cs_3Sb. The excited electrons closing to the depletion region (or in the depletion region) diffuse toward the substrate side in all cases; thus, the quantum efficiency of the Cs_3Sb cathode on all substrates is the same. The difference in the conduction-band minimum between Cs_3Sb and the substrates do not make affect the QE.

These results can be explained in a unified manner by the energy-band models for semiconductor(metal)-semiconductor junction between the cathode and the

substrates. It indicates that, in order to obtain a high QE, the conduction-band minimum of the substrate should be higher than that of the cathode.

IV. SUMMARY

We studied the substrate dependence of the performance of the CsK₂Sb photocathode by employing an evaporation process which gives high QE with high reproducibility. We found that the cathodes on *p*-GaAs(100), *p*-Si(100), and Mo(100) had significantly higher QE values than those on *n*-GaAs(100) and *n*-Si(100). We also found that Cs₃Sb did not depend on the *pn*-type. These results clearly show that the cathode performance depends not only on the substrate material, surface state, and surface orientation, but also the *pn*-type. When the conduction-band minimum of the substrate is higher than that of the cathode, we can obtain high QE. This finding indicates a possibility of improving the thin-film cathode performance by choosing a suitable combination between the cathode and the substrate.

ACKNOWLEDGMENTS

[1] H. Abe, S. Adachi, K. Amemiya, T. Arima, K. Asakura *et al.*, ERL conceptual design report, KEK Report No. 2012-4, 2012.

[2] M. Altarelli, R. Brinkmann, M. Chergui, W. Decking, B. Dobson *et al.*, The European X-ray Free Electron Laser technical design report, Report No. DESY 2006-97, 2006.

[3] International Linear Collider Techinical Design Report, see http://www.linearcollider.org/ILC/Publications/Technical-Design-Report.

[4] J. N. Galayda (LCLS-II Collaboration), The Linac Coherent Light Source-II Project, *Proceedings of IPAC2014, Dresden, Germany* (JACoW, Dresden, Germany, 2014), pp. 935–937, TUOCA01, http://accelconf.web.cern.ch/AccelConf/IPAC2014/papers/tuoca01.pdf.

[5] E. Chevallay, J. Durand, S. Hutffchins, G. Suberlucq, and M. Wurgel, Photocathodes tested in the dc gun of the CERN photoemission laboratory, Nucl. Instrum. Methods Phys. Res., Sect. A **340**, 146 (1994).

[6] P. G. O'Shea, High-brightness rf photocathode guns for single pass X-ray free-electron lasers, Nucl. Instrum. Methods Phys. Res., Sect. A **358**, 36 (1995).

[7] A. K. Pandey, P. E. Shaw, I. D. W. Samuel, and J.-M. Nunzi, Effect of metal cathode reflectance on the exciton-dissociation efficiency in heterojunction organic solar cells, Appl. Phys. Lett. **94**, 103303 (2009).

[8] V. G. Dmitriev, G. G. Gurzadyan and D. N. Nikogosyan, *Handbook of Nonlinear Optical Crystals* (Springer-Verlag New York, 1995).

[9] https://www.hamamatsu.com/jp/en/product/optical-sensors/pmt/index.html.

[10] A. H. Sommer, *n*-Type and *p*-Type Conduction in Alkali-Antimonide Photoemitters, J. Appl. Phys. **29**, 1568 (1958).

[11] H.-S. Jeong, Electron emission properties of Cs₃Sb photocathode emitters in a panel device, J. Vac. Sci. Technol. B **33**, 031214 (2015).

[12] D. G. Fisher, A. F. McDonie, and A. H. Sommer, Band-bending effects in Na₂KSb and K₂CsSb photocathodes, J. Appl. Phys. **45**, 487 (1974).

[13] M. A. Nichols, Preparation/characterization of atomically flat and clean Mo (100) surfaces and thermal emittance/response time measurements of Cs₃Sb photocathodes, University of California Report No. 94720, 2011, https://pdfs.semanticscholar.org/4406/7692e9586008d440f9808dfb147e58e5cb1e.pdf.

[14] S. Karkare, I. V. Bazarov, L. E. Boulet, M. Brown, L. Cultrera *et al.*, in *Proceedings of the 25th Particle Accelerator Conference, PAC-2013, Pasadena, CA, 2013* (IEEE, New York, 2013), TUOAB1.

[15] L. Cultrera, I. V. Bazarov, J. V. Conway, B. Dunham, S. Karkare *et al.*, in *Proceedings of the 24th Particle Accelerator Conference, PAC-2011, New York, 2011* (IEEE, New York, 2011), WEP244.

[16] I. Pinayev, V. N. Litvinenko, J. Tuozzolo, J. C. Brutus, S. Belomestnykh *et al.*, High-gradient high-charge CW superconducting rf gun with CsK2Sb photocathode, arXiv:1511.05595.

[17] T. Vecchione, I. Ben-Zvi, D. H. Dowell, J. Feng, T. Rao, J. Smedley, W. Wan, and H. A. Padmore, A low emittance and high efficiency visible light photocathode for high brightness accelerator-based X-ray light sources, Appl. Phys. Lett. **99**, 034103 (2011).

[18] A. Burrill, I. Ben-Zvi, T. Rao, D. Pate, Z. Segalov, and D. Dowell, in *Proceedings of the 21st Particle Accelerator Conference, Knoxville, TN, 2005* (IEEE, Piscataway, NJ, 2005), p. 2672.

[19] M. Kuriki, A Yokota, K. Negishi, R. Kaku, and M. Urano, A study of operational lifetime of CsK₂sb photo-cathode, *Proceedings of IPAC2016, Busan, Korea* (CERN, Busan, Korea, 2016), pp. 3938–3940, THPOW006, http://accelconf.web.cern.ch/accelconf/ipac2016/papers/thpow006.pdf.

[20] S. Valeri, M. G. Lancellotti, C. Mariani, A. Di Bona, P. Michelato, C. Pagani, and M. Sancrotti, in *Proceedings of the 4th European Particle Accelerator Conference, London, England, 1994* (EPS-AG, London, UK, 1994), pp. 1459.

[21] S. Schubert, J. Smedley, T. Rao, M. Ruiz-Oses, X. Liang, I. Ben-Zvi, H. Padmore, and T. Vecchione, in *Proceedings of the 4th International Particle Accelerator Conference, IPAC-2013, Shanghai, China, 2013* (JACoW, Shanghai, China, 2013), MOPFI005.

[22] M. Ruiz-Oses, S. Schubert, K. Attenkofer, I. Ben-Zvi, X. Liang *et al.*, Direct observation of bi-alkali antimonide photocathodes growth via in operando x-ray diffraction studies, APL Mater. **2**, 121101 (2014).

[23] S. Schubert, J. Wong, J. Feng, S. Karkare, H. Padmore *et al.*, Bi-alkali antimonide photocathode growth: An X-ray diffraction study, J. Appl. Phys. **120**, 035303 (2016).

[24] Z. Ding, S. Karkare, J. Feng, D. Filippetto, M. Johnson *et al.*, Temperature-dependent quantum efficiency degradation of *K*-Cs-Sb bialkali antimonide photocathodes

grown by a triple-element codeposition method, Phys. Rev. Accel. Beams **20**, 113401 (2017).

[25] J. Feng, S. Karkare, J. Nasiatka, S. Schubert, J. Smedley, and H. Padmore, Near atomically smooth alkali antimonide photocathode thin films, J. Appl. Phys. **121**, 044904 (2017).

[26] L. Guo, M. Kuriki, A. Yokota, M. Urano, and K. Negishi, Substrate dependence of CsK_2Sb photo-cathode performance, Prog. Theor. Exp. Phys. (**2017**) 033G01.

[27] K. Reinhardt and W. Kern, *Handbook of Silicon Wafer Cleaning Technology*, 2nd ed. (William Andrew, Norwich, NY, 2008).

[28] O. E. Tereshchenko, S. I. Chikichev, and A. S. Terekhov, Atomic structure and electronic properties of HCl–isopropanol treated and vacuum annealed GaAs(100) surface, Appl. Surf. Sci. **142**, 75 (1999).

[29] L. Cultrera, H. Lee, and I. Bazarov, Alkali antimonides photocathodes growth using pure metals evaporation from effusion cells, J. Vac. Sci. Technol. B **34**, 011202 (2016).

[30] L. Cultrera, I. Bazarov, A. Bartnik, B. Dunham, S. Karkare, R. Merluzzi, and M. Nichols, Thermal emittance and response time of a cesium antimonide photocathode, Appl. Phys. Lett. **99**, 152110 (2011).

[31] C. Ghosh and B. P. Varma, Preparation and study of properties of a few alkali antimonide photocathodes, J. Appl. Phys. **49**, 8 (1978).

[32] S. Schubert, H. Padmore, J. Wong, Z. Ding, M. Gaowei *et al.*, *Proceedings of IPAC2015, Richmond, VA, USA* (JACoW, Richmond, VA, USA, 2015), p. 371, WEPWA032, http://accelconf.web.cern.ch/AccelConf/IPAC2015/papers/wepwa032.pdf.

[33] R. A. Loch, Cesium-Telluride and Magnesium for high quality photocathodes, Masterdiploma thesis, University of Twente, 2005.

[34] Electrostatic analysis of a $p-n$ diode, https://ecee.colorado.edu/~bart/book/book/chapter4/ch4_3.htm.

[35] H.-S. Jeong, K. Keller, and B. Culkin, Electron emission properties of Cs_3Sb photocathode emitters in a panel device, J. Vac. Sci. Technol. B **33**, 031214 (2015).